Pre- and postexposure efficacy of fully human antibodies against Spike protein in a novel humanized mouse model of MERS-CoV infection

Kristen E. Pascal[a,1], Christopher M. Coleman[b,1], Alejandro O. Mujica[a], Vishal Kamat[a], Ashok Badithe[a], Jeanette Fairhurst[a], Charleen Hunt[a], John Strein[a], Alexander Berrebi[c], Jeanne M. Sisk[b], Krystal L. Matthews[b], Robert Babb[a], Gang Chen[a], Ka-Man V. Lai[a], Tammy T. Huang[a], William Olson[a], George D. Yancopoulos[a,2], Neil Stahl[a], Matthew B. Frieman[b,3], and Christos A. Kyratsous[a,2,3]

[a]Regeneron Pharmaceuticals, Inc., Tarrytown, NY 10591; [b]Department of Microbiology and Immunology, University of Maryland School of Medicine, Baltimore, MD 21201; and [c]Department of Pathology, University of Maryland School of Medicine, Baltimore, MD 21201

Contributed by George D. Yancopoulos, June 2, 2015 (sent for review March 16, 2015; reviewed by Marcel A. Müller)

Traditional approaches to antimicrobial drug development are poorly suited to combatting the emergence of novel pathogens. Additionally, the lack of small animal models for these infections hinders the in vivo testing of potential therapeutics. Here we demonstrate the use of the VelocImmune technology (a mouse that expresses human antibody-variable heavy chains and κ light chains) alongside the VelociGene technology (which allows for rapid engineering of the mouse genome) to quickly develop and evaluate antibodies against an emerging viral disease. Specifically, we show the rapid generation of fully human neutralizing antibodies against the recently emerged Middle East Respiratory Syndrome coronavirus (MERS-CoV) and development of a humanized mouse model for MERS-CoV infection, which was used to demonstrate the therapeutic efficacy of the isolated antibodies. The VelocImmune and VelociGene technologies are powerful platforms that can be used to rapidly respond to emerging epidemics.

MERS-CoV | Spike | DPP4 | neutralizing antibody | mouse model

Middle East respiratory syndrome coronavirus (MERS-CoV) was first isolated in September 2012 in the Kingdom of Saudi Arabia (1). Since then, more than 1,100 cases and more than 422 deaths have been reported in the Middle East (Iran, Jordan, Kuwait, Lebanon, Oman, Qatar, Saudi Arabia, United Arab Emirates, and Yemen), in Africa (Algeria, Egypt and Tunisia), in Europe (Austria, France, Germany, Greece, Italy, the Netherlands, and the United Kingdom), in Asia (Malaysia and Philippines), and in the United States of America (www.who.int/csr/disease/coronavirus_infections/archive_updates/en/) as of April 29, 2015. Clinical features of MERS-CoV infection in humans range from an asymptomatic infection to very severe pneumonia, with potential development of acute respiratory distress syndrome, shock, and multiorgan failure, resulting in death (2).

MERS-CoV is a betacoronavirus related to the severe acute respiratory syndrome coronavirus (SARS-CoV). Both viruses cause severe respiratory tract infections and are associated with high mortality rates. Although human-to-human transmission of MERS-CoV has been reported (3), the rate of transmission appears to be low (4, 5). Recent studies have suggested that dromedary camels are involved in the zoonotic transmission of MERS-CoV; analyses of camel sera indicate MERS-CoV seropositivity in camels throughout the Middle East and Africa, suggesting MERS-CoV maintenance in camel populations (6–8).

The MERS-CoV virion is decorated with a class I transmembrane envelope protein named Spike (S). S protein forms a homo-trimer and mediates binding to host receptors, membrane fusion, and entry into susceptible cells (9); consistent with this, MERS-CoV S protein is a major target for neutralizing antibodies (10). The receptor for MERS-CoV was identified as dipeptidyl peptidase 4 (DDP4, also known as CD26) (11), a protein with diverse functions in glucose homeostasis, T-cell activation, neurotransmitter function, and modulation of cardiac signaling (12). DPP4 is expressed in a variety of cell types, including endothelial cells, hepatocytes, enterocytes, and cells of the renal glomeruli and proximal tubules (12). Moreover, DPP4 recognition is mediated by the receptor-binding doman (RBD, amino acids E367–Y606), and the structural basis for this interaction was recently delineated (13, 14).

Currently, there are no approved treatments or vaccines to treat or prevent MERS-CoV infections. Type I IFN and ribavirin have been reported to ameliorate disease in infected macaques (15), and small molecules targeting diverse intracellular pathways have been shown to inhibit MERS-CoV in vitro (16–18). Furthermore, experimental immunogens can elicit an anti–MERS-CoV response (19, 20). However, no MERS-CoV targeting therapeutic has been demonstrated to function in vivo, partly because of limited small animal models of infection (21–23). MERS-CoV does not natively replicate in wild-type mice.

Significance

Traditional approaches for development of antibodies are poorly suited to combating the emergence of novel pathogens, as they require multiple steps of laborious optimization and process adaptation for clinical development. Here, we describe the simultaneous use of two state-of-the-art technologies to rapidly generate and validate antibodies against Middle East Respiratory Syndrome coronavirus (MERS-CoV), following a highly optimized process that links immunization to production of clinical material grade antibodies and developed promising clinical candidates for prophylaxis and treatment of MERS-CoV, and a humanized mouse model of infection that was used to evaluate our therapeutics. This study forms the basis for a rapid response to address the public threat resulting from emerging coronaviruses or other pathogens that pose a serious threat to human health in the future.

Author contributions: A.O.M., A. Badithe, R.B., G.C., K.-M.V.L., T.T.H., W.O., G.D.Y., N.S., M.B.F., and C.A.K. designed research; K.E.P., C.M.C., V.K., J.F., C.H., J.S., A. Berrebi, J.M.S., K.L.M., and M.B.F. performed research; K.E.P., C.M.C., A.O.M., V.K., A. Badithe, J.F., R.B., G.C., K.-M.V.L., T.T.H., W.O., G.D.Y., N.S., M.B.F., and C.A.K. analyzed data; and C.M.C., M.B.F., and C.A.K. wrote the paper.

Reviewers included: M.A.M., University of Bonn Medical Centre.

Conflict of interest statement: K.E.P., A.O.M., V.K., A.B., J.F., C.H., J.S., R.B., G.C., K.-M.V.L., T.T.H., W.O., G.D.Y., N.S., and C.A.K. are employees of Regeneron Pharmaceuticals, Inc. The work was funded by Regeneron Pharmaceuticals, Inc.

Freely available online through the PNAS open access option.

[1]K.E.P. and C.M.C. contributed equally to this work.

[2]To whom correspondence may be addressed. Email: george@regeneron.com or christos.kyratsous@regeneron.com.

[3]M.B.F. and C.A.K. contributed equally to this work.

This article contains supporting information online at www.pnas.org/lookup/suppl/doi:10.1073/pnas.1510830112/-/DCSupplemental.

Two mouse models have been developed. In the first, a modified adenovirus expressing huDPP4 is administered intranasally to mice leading to huDPP4 expression in all cells of the lung, not just those that natively express DPP4 (21). In this model, mice show transient huDPP4 expression and mild lung disease. In the second model (23), a transgenic mouse was produced that expresses huDPP4 in all cells of the body, which in not physiologically relevant. In this model, MERS-CoV infection leads to high levels of viral RNA and inflammation in the lungs, but also significant inflammation and viral RNA in the brains of infected mice. However, no previous reports have documented tropism of MERS-CoV to the brains of an infected host, suggesting that studying pathogenesis of MERS-CoV in this model is limited. Therefore, there is a need for development of physiologically relevant small animal models to study MERS-CoV pathogenesis, as well as to test anti–MERS-CoV therapeutics in vivo.

Here we use the VelocImmune platform to rapidly generate a panel of fully human, noncompeting monoclonal antibodies that bind to MERS-CoV S protein and inhibit entry into target cells. We show that two of these antibodies can potently neutralize pseudoparticles generated with all clinical MERS-CoV S RBD variants isolated to date. Importantly, we demonstrate that the fully human VelocImmune antibodies neutralize infectious MERS-CoV significantly more than published monoclonals isolated using traditional methods. Finally, we used the VelociGene technology to develop a novel humanized model for MERS-CoV infection and showed that our antibodies can prevent and treat MERS-CoV infection in vivo. Our antibodies are, to our knowledge, the first anti–MERS-CoV fully human antibodies to block MERS-CoV infection in vivo and are promising therapeutic candidates. Importantly, we demonstrate the value of the VelocImmune and VelociGene platforms for the rapid generation and validation of therapeutic antibodies against emerging viral pathogens.

Results

Isolation and Characterization of Anti–MERS-CoV Spike Protein Antibodies. VelocImmune mice were immunized with DNA encoding for MERS-CoV S protein and recombinant purified S protein and polyclonal titers were monitored. When sufficient responses were observed, spleens were harvested and monoclonal antibodies were isolated by both conventional hybridoma methodology and B-cell sorting technology. Supernatants containing antibodies were screened, as outlined in Fig. S1. To enrich for antibodies that could block the binding of its S protein to its receptor DPP4 and then potentially neutralize MERS-CoV, we tested more than 1,000 supernatants for binding to purified MERS-CoV-S-RBD (13). A blocking ELISA was then used to screen for antigen-positive supernatants that were able to block the interaction between MERS-CoV-S-RBD and DPP4. The ability of these antibodies to block entry of retrovirus particles pseudotyped with MERS-CoV S protein (MERSpp) was then quantified. All lead antibodies were subsequently cloned on to hIgG1 Fc regions, sequenced, expressed in CHO cells, and purified for further characterization. Using these methods, we identified approximately 30 fully human monoclonal antibodies that can very potently neutralize MERS-CoV by blocking the S protein–DPP4 interaction.

Although betacoronaviruses have lower mutation rates compared with other RNA viruses (24), they can still rapidly generate mutants and escape the pressure of a single therapeutic agent, including monoclonal antibodies (25–27). Therefore, we sought to isolate blocking antibodies that do not cross-compete for binding to MERS-CoV S protein and thus could be used together as a antibody mixture that is less susceptible to virus escape. To this end, we monitored the binding kinetics of each of the purified antibodies on MERS-CoV S protein precomplexed with a second antibody to select for pairs that do not cross-compete with each other. Based on the data presented in Fig. S2 *A* and *B* and Table S1, we conclude that REGN3048 and REGN3051 can cobind MERS-CoV RBD, suggesting that the two antibodies bind to discrete epitopes. Mutation of one epitope as a result of selective pressure by one antibody should not affect binding of the other antibody.

REGN3051 and REGN3048 were selected as the two lead antibodies that met all of the screening criteria.

REGN3051 and REGN3048 Bind to MERS-CoV RBD with High Affinity. To determine the binding kinetics of our monoclonal antibodies to MERS-CoV-RBD protein, surface plasmon resonance Biacore studies were performed (Fig. S2 *C* and *D*). The complete kinetic binding parameters for REGN3048 and REGN3051 are shown in Table S2. Both antibodies exhibit tight binding to the recombinant S protein with equilibrium dissociation constant (K_D) values ranging from 43–48 pM at 37 °C, suggesting that they have a high affinity for binding to MERS-CoV S protein.

Neutralization of MERS-CoV Pseudovirus and Infectious Virus by REGN3051 and REGN3048. The neutralization activities of REGN3051 and REGN3048 were first evaluated using MERSpp that express a luciferase reporter. These particles were incubated with decreasing concentrations of REGN3051 and REGN3048. Huh-7 cells were then transduced with the MERSpp/antibody complexes and intracellular luciferase activity was measured 3 d later. As seen in Fig. 1*A*, both antibodies can block cell entry of the pseudoparticles at picomolar concentrations; the 50% inhibitory concentration (IC_{50}) was 65 pM and 70 pM for REGN3051 and REGN3048, respectively. The entry of MERSpp was not affected by an isotype control antibody used at up to 10-fold higher concentrations. Importantly, the neutralization activity of these antibodies was specific for MERSpp, as neither inhibited the entry of control pseudoparticles [vesicular stomatitis virus glycoprotein (VSVg) pseudotyped particles] (Fig. 1*B*).

We next tested the ability of these two monoclonal antibodies to neutralize live MERS-CoV virus in vitro. Decreasing concentrations of antibodies were incubated with a defined amount of the clinical isolate MERS-CoV strain EMC/2012 (1). Vero E6 cells were then infected with the mixture and cell-viability was measured 2 d later. As shown in Fig. 1*C*, both REGN3051 and

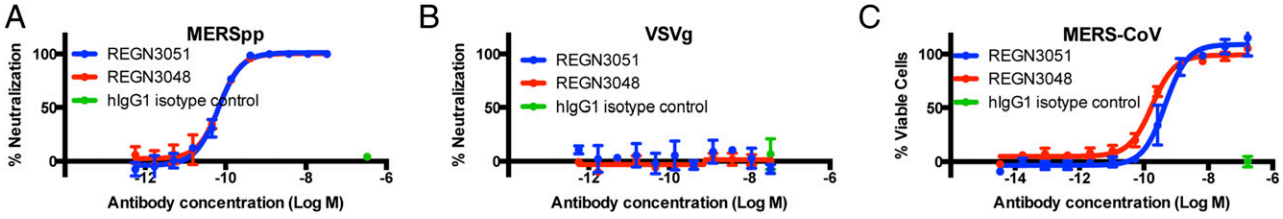

Fig. 1. MERS-CoV pseudotype and live MERS-CoV is neutralized by REGN3048 and REGN3051 in vitro. Luciferase expressing particles pseudotyped with either MERS-CoV S (*A*) or VSV-G (*B*) were incubated with either antibody at the indicated concentrations and the mix was used to transduce Huh-7 cells. At 72 h postinfection, luciferase was measured. Percent neutralization was calculated as the ratio of luciferase signal relative to no nontransduced and nonantibody-treated controls. (*C*) Live MERS-CoV was premixed with each noted antibody and used to infect cells across a dose range of each antibody. At 48 h postinfection, cells were analyzed for viability. Percent survival is graphed as a measure of MERS-CoV replication leading to cell death.

REGN3048 exhibited potent inhibitory activity against MERS-CoV, with IC_{50} values of 460 pM and 180 pM, respectively.

Taken together, these data suggest that REGN3051 and REGN3048 potently block entry of MERS-CoV into susceptible cell lines and neutralize infectivity.

Breadth of MERS-CoV Neutralization by REGN3051 and REGN3048. RNA viruses encode a low-fidelity genome replication machinery that allows them to rapidly adapt to their host environment (28). However, coronaviruses, such as MERS-CoV, encode for a nonstructural protein with a 3′-to-5′ exo-ribonuclease activity, which provides a proof-reading function during their replication and greatly increases the coding capacity of the genome without leading to mutational catastrophe (29, 30). Despite that finding, sequencing of multiple clinical isolates sampled during the first 2 y of the MERS-CoV epidemic has revealed that the MERS-CoV S protein of the virus is evolving (4, 31). We aligned 38 National Center for Biotechnology Information deposited sequences of MERS-CoV clinical isolates and compared them to the sequence of the first isolated strain, EMC/2012 (1). Based on the design of our screening assay, both REGN3051 and REGN3048 are expected to bind within the RBD of the MERS-CoV S protein, so the comparison of the sequences specifically focused on amino acids 367–606. We identified seven different amino acids that differ between the sequenced clinical isolates and the prototype EMC/2012 sequence: A431P, S457G, S460F, A482V, L506F, D509G, and V534A (Table S3). To test the ability of our antibodies to bind to conserved regions within the RBD and neutralize all MERS-CoV clinical isolates sequenced as of July 2014, we used site-directed mutagenesis to create plasmid constructs encoding for all S protein variants. We then used these to generate MERSpp pseudotyped with the modified S proteins and performed neutralization assays. REGN3051 is able to neutralize all isolates with IC_{50} values ranging from 13–65 pM (Fig. S3). Similar values were also observed for REGN3048, with the exception of the V534A variant, which exhibited a partial resistance to the antibody. It is worth noting however, that this amino acid change was only observed in a single MERS-CoV isolate (Riyadh_2), which was isolated in 2012 and is part of a dead branch of the MERS-CoV evolutionary tree (31).

These data suggest that REGN3051 and REGN3048 bind to regions of MERS-CoV S protein that are conserved during the natural evolution of the virus.

REGN3051 and REGN3048 Are More Effective Neutralizers than Previously Isolated MERS-CoV Monoclonal Antibodies. We next compared the potency of our two antibodies with previously isolated monoclonal antibodies. Three groups have used in vitro antibody isolation methods—that is, phage display (26, 27) and yeast display (32)—to select for antibodies that bind to MERS-CoV S protein and block virus entry. For our studies, we selected a panel of three antibodies with published variable domain sequences, which were reported to potently neutralize MERS-CoV and bind to diverse epitopes. The published sequences for antibodies 3B12, MERS-4, and MERS-27 (27, 32) were cloned onto human IgG1 constant domains, then expressed and purified similarly to REGN3051 and REGN3048. We tested the three purified antibodies for binding to MERS S protein, blockade of the S protein–DPP4 interaction, and published neutralization properties (Fig. S3). We then tested the neutralization efficacy of all five antibodies using pseudoparticles generated with the prototypical EMC/2012 sequence and all clinical isolates described above (Fig. S3). REGN3051 and REGN3048 neutralize MERSpp with IC_{50} values at least one log lower than the most potent comparator antibody, MERS-4. In addition, both 3B12 and MERS-27 appear to bind to less conserved sites on the MERS-CoV S protein, as pseudoparticles with sequences of multiple clinical isolates cannot be neutralized with these antibodies. These data suggest that antibodies isolated after in vivo selection using the VelociImmune platform are able to neutralize a broader range of MERS-CoV isolates with improved potency compared with several antibodies isolated solely based on in vitro biochemical properties.

Humanized Mice for DPP4 Are Susceptible to MERS-CoV Infection. In vivo testing of antiviral molecules requires a small animal model that is susceptible to MERS-CoV infection; however, wild-type mice are not susceptible to MERS-CoV infection (33). Sequence comparison of the sequence of mouse and human DPP4 revealed that the amino acids that have previously been identified as contact sites between MERS-CoV S protein and its receptor (13) differ between the two species. In addition, expression of human DPP4 in mouse cells allows for MERSpp entry and MERS-CoV propagation (34), indicating that entry of the virus is the limiting step in infection of mouse cells.

We hypothesized that mice expressing human DPP4 in place of mouse DPP4 would be susceptible to MERS-CoV and allow for in vivo testing of anti–MERS-CoV therapeutics. We used VelociGene technology to replace the 79 kb of the mouse *Dpp4* gene with 82 kb of its human ortholog (Fig. S4*A*). The resulting mice express fully human DPP4 under the control of the mouse regulatory elements, to preserve the proper expression regulation and protein tissue distribution. Immunohistochemistry was performed to confirm huDPP4 expression in the lungs of huDPP4 mice. Using an antibody specific for huDPP4, we detected huDPP4 expressed in club cells, type 2 alveolar epithelial cells, and alveolar macrophages (Fig. S4*B*).

To test if humanized DPP4 mice (huDPP4 mice) can support infection, we intranasally inoculated mice with 2×10^5 pfu of MERS-CoV. Although no mortality or clinical signs of disease was observed up to day 4, at days 2 and 4 postinfection mice were killed and their lungs were dissected. To obtain virus RNA levels, lungs were homogenized and analyzed by real-time PCR using primers specific to MERS-CoV (Fig. 2 *A* and *B*). To obtain virus titers, lungs were homogenized, clarified by centrifugation, and titered (Fig. 2*C*). Robust MERS-CoV replication in the lungs was evident at 2 and 4 d postinfection (dpi). RNA quantification, using primer sets specific for the MERS-CoV genome and

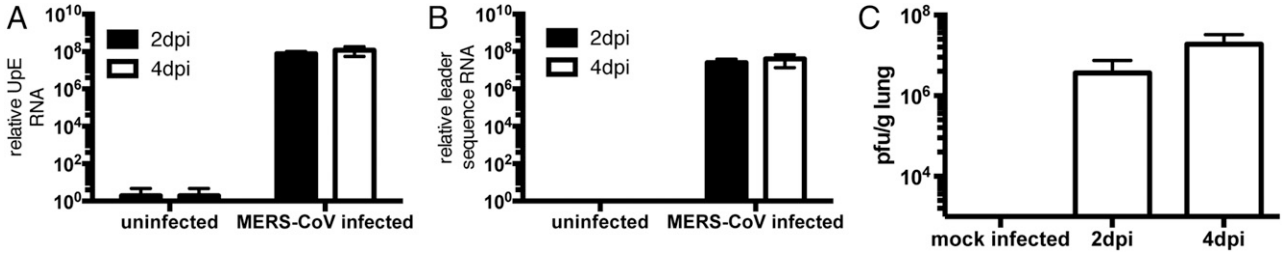

Fig. 2. Transgenic huDPP4-containing mice and pathogenesis characterization. (*A* and *B*) Quantitative PCR of MERS-CoV transcript (*A* is MERS-CoV transcribed mRNA, *B* is MERS-CoV genome) in infected mice at days 2 and 4 postinfection ($n = 5$ mice per time point). (*C*) MERS-CoV viral titer quantitation of infected mouse lung at day 4 postinfection. Mouse lung MERS-CoV levels quantified by TCID50 assay and expressed as plaque-forming unit per gram of homogenized mouse lung ($n = 5$ mice per time point).

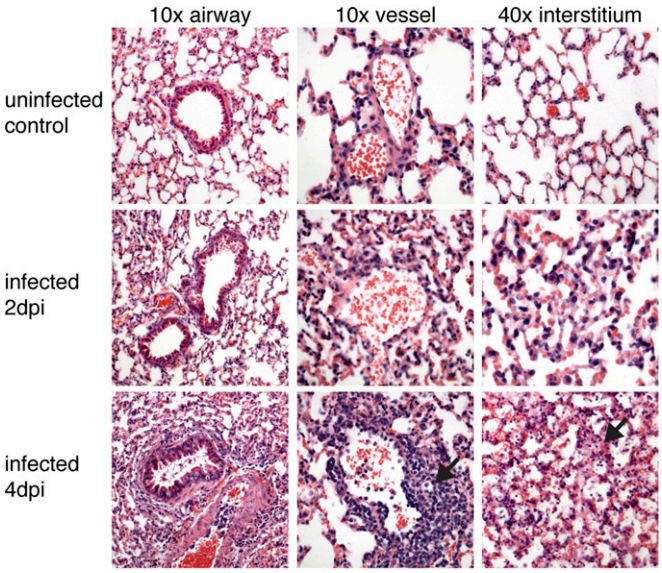

Fig. 3. MERS-CoV pathogenesis in huDPP4 mice. H&E staining of mouse lung from MERS-CoV infected mice. Airway (10× magnification), vasculature (10× magnification), and interstitium (40× magnification) are shown for PBS, day 2 and day 4 postinfection mice (representative images of five mice at each time point).

MERS-CoV leader (designed to only amplify replicating MERS-CoV), demonstrated high levels of MERS-CoV replicating RNA in lungs collected at day 2, and these levels were maintained through day 4 postinfection. Plaque assay of lung homogenate quantified MERS-CoV levels of ~3.63×10^6 pfu/g lung at day 2 and ~1.88×10^7 pfu/g lung at 4 dpi, demonstrating active replication of MERS-CoV in the lungs of the huDPP4 mice. These data suggest that humanization of DPP4 using VelociGene technology has created a robust model of MERS-CoV in mice that can be used to assess MERS-CoV treatment in vivo.

Lungs from huDPP4 mice intranasally inoculated with either MERS-CoV or sham infected with PBS were analyzed for pathological changes (Fig. 3). At day 2 postinfection, peribronchiolar inflammation was evident with alterations in bronchiolar cell structure found throughout the lungs. Minimal perivascular inflammation or effects on alveolar structures were noted at day 2 postinfection. At 4 dpi, significant interstitial infiltration was observed with peri-vascular cuffing and extensive alveolar thickening. Bronchiolar alterations were still present as well. Importantly, this lung pathology is consistent with the radiographic findings of development of interstitial pneumonia and significant lung disease seen in humans with MERS-CoV, suggesting that this humanized DPP4 in vivo model of MERS-CoV infection recapitulates pathological sequelae that are seen in MERS-CoV infection of humans.

Unlike what is seen with other mouse models of MERS-CoV infections, virus replication and pathology in the huDPP4 mice is localized in the lungs. Histological analysis of brains section 4 dpi demonstrated no inflammation (Fig. S5). Homogenate of brain from MERS-CoV infected huDPP4 mice was tested for MERS-CoV specific mRNA at both day 2 and day 4 postinfection. No MERS-CoV specific RNA was detected.

REGN3051 and REGN3048 Protect huDPP4 Mice from MERS-CoV Infection. Having established that humanized DPP4 mice were susceptible to MERS-CoV, we used this model to evaluate the activity of REGN3051 and REGN3048 in vivo. Mice were intraperitoneally injected with 200, 20, or 2 μg of either REGN3051, REGN3048, or 200 μg of hIgG1 isotype control antibody 24 h before intranasal infection with 1×10^5 pfu of MERS-CoV. As seen in Fig. 4 *A* and *B*, both REGN3051 and REGN3048 were able to significantly decrease MERS-CoV specific RNA levels in the lungs by over 2 logs at the 200 μg per mouse dose, compared with the isotype control antibody. REGN3051 was more effective at reducing MERS-CoV RNA levels at the 20-μg dose compared with REGN3048 at the same dose. The 2-μg dosing of either antibody was ineffective at reducing viral RNA levels compared with isotype control-treated mice. When MERS-CoV titer was analyzed in the lungs (Fig. 4*C*) we found that both the 200- and 20-μg dose of REGN3051 reduces virus levels to near the level of detection in the assay (1×10^5 pfu/g). REGN3048 is equally efficient at the 200-μg dose as REGN3051, whereas the 20- and 2-μg display a dose dependent inhibition of viral inhibition. These data suggest that REGN3051 and REGN3048 can effectively block MERS-CoV infection in vivo.

Histological analysis was also performed on lungs from mice treated 24 h preinfection with REGN3048, REGN3051, or hIgG1 isotype control antibody at 4 dpi (Fig. S6*A*). Lungs from mice pretreated with hIgG isotype control mice displayed significant lung pathology with increased interstitial inflammation, perivascular cuffing, and thickening of alveolar septa. Mice treated with 200 μg of either REGN3048 or REGN3051 had reduced inflammation with minimal foci of inflammatory cells in the interstitium and minor bronchiolar cuffing. In mice pretreated with 20 μg of REGN3048 and REGN3051, we found moderate levels of perivascular cuffing and interstitial inflammation compared with the higher antibody group. In contrast, the 2-μg

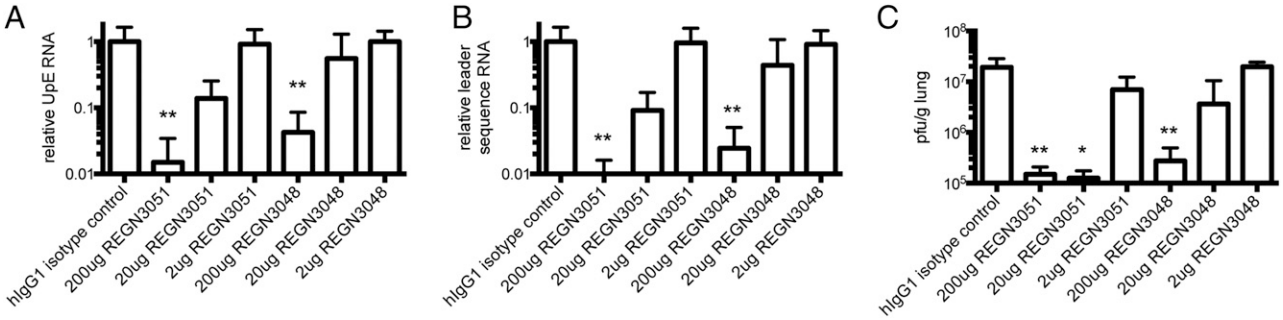

Fig. 4. In vivo treatment with anti-S antibodies one day before infection protects huDPP4 mice from MERS-CoV infection. Mice were intraperitoneally injected with a dose range of REGN3051 and REGN3048 monoclonal antibodies at 24 h preinfection with MERS-CoV. At 4 dpi, lungs were harvested and viral RNA and virus titer quantified. (*A* and *B*) Quantitative PCR of MERS-CoV transcript (*A* is MERS-CoV genome, *B* is MERS-CoV transcribed mRNA) from infected lungs was quantified using primers directed against the MERS-CoV genome and compared with hIgG1 isotype control-treated mice. All samples were compared with hIgG1 control ($n = 5$ mice per time point and quantitative PCR performed in triplicate). (*C*) Analysis of viral titer in the lungs quantitated by plaque assay reported as plaque-forming unit per gram lung ($n = 5$ mice per time point and titers performed in triplicate). *$P < 0.05$ and **$P < 0.01$.

antibody pretreated group had similar pathology to the hIgG1 isotype control displaying significant interstitial inflammation and predominant peri-vascular inflammation. Blinded histological scoring (Fig. S6*B*) reflects the reduced inflammation scores for treated mice. These data demonstrate that REGN3048 and REGN3051 confer a dose-dependent reduction in lung pathology following MERS-CoV infection corroborating viral RNA levels and virus titers determined for these mice.

Taken together, these data indicate that REGN3051 and REGN3048 can block MERS-CoV infection and disease in vivo when injected 1 d before infection. To our knowledge, REGN3051 and REGN3048 are, to our knowledge, the first fully human antibodies that have been shown to display efficacy in an in vivo model of MERS-CoV infection.

REGN3051 and REGN3048 Can Treat Humanized DPP4 Mice Infected with MERS-CoV. The ability to inhibit MERS-CoV replication and lung pathology after infection is a desired trait in a potential therapeutic. To assess whether REGN3051 is able have an effect therapeutically, we infected huDPP4 mice with MERS-CoV, and then 24 h later injected the infected mice intraperitoneally with either 500 μg of hIgG isotype control or REGN3051 at 500 or 200 μg per mouse. At 4 dpi, mice were killed and mouse lungs were analyzed for viral RNA, virus titer, and lung pathology. Both the 500- and 200-μg doses of REGN3051 were able to reduce viral RNA levels by about 10-fold in the lungs of mice compared with control antibody treated mice (Fig. 5 *A* and *B*). Lung titers of the same mice demonstrated significant reduction in MERS-CoV levels in the lungs with a greater than 2 log reduction at day 4 postinfection (Fig. 5*C*). These data demonstrate that REGN3051 can significantly inhibit viral replication even when administered 24 h following viral inoculation.

Histological analysis was performed on mice treated 24 h postinfection with hIgG control antibody, 500 μg REGN3051, or 200 μg REGN3051 (Fig. S7*A*). Mice treated with control antibody displayed similar pathology to the control above with significant interstitial inflammation, peri-vascular cuffing and thickening of alveolar septa. Mice treated with either 200 or 500 μg of REGN3051 had minimal interstitial inflammation and with reduced and only focal peri-vascular inflammation throughout the lungs. Blinded histological scoring demonstrates reduced inflammation scores for treated mice (Fig. S7*B*). These data demonstrate that therapeutic doses of REGN3051 reduce MERS-CoV induced lung pathology even when given 24 h postinfection.

Taken together, these data demonstrate that by coupling our VelocImmune and VelociGene technologies, we were able to rapidly produce candidate monoclonal antibodies and rapidly create relevant mouse models that were useful to evaluate potential therapeutics to prevent or treat infections by an emerging infectious disease threat.

Discussion

Passive immunotherapy for prophylaxis or treatment of infectious diseases has been used for more than a century, usually in the form of convalescent human sera that contains high titers of neutralizing antibodies (35). Today, multiple purified monoclonal antibodies are currently in preclinical and clinical development for use as antimicrobials (36).

In this report, we describe the generation of two fully human antibodies (REGN3051 and REGN3048), which bind to the MERS-CoV RBD, block the interaction of the S protein with its cellular receptor DPP4, and very potently neutralize MERS-CoV infectivity in vitro. REGN3051 and REGN3048 do not cross-compete for binding on MERS-CoV S protein, and therefore may potentially be used together as a mixture to reduce the ability of MERS-CoV to escape via mutation in response to the selective pressure from either component. Importantly, these antibodies bind to epitopes on the S protein that have been conserved during the natural evolution of the virus during the past 2 y. The development of these molecules followed a highly optimized process that links direct isolation of antibodies from B cells to development of isogenic cell lines expressing our antibodies. Following this procedure we were able within only 6 wk to proceed from antibody selection to purification of gram quantity of protein amounts to allow for further in vitro and in vivo characterization. Importantly, the cell lines that were used for every one of these steps have predictable bioreactor properties and can immediately be used for production of clinical grade antibody material.

In addition, we developed a novel transgenic mouse model that supports MERS-CoV infection by replacing the mouse DPP4 coding sequence with that encoding human DPP4. Using the VelociMouse method, F0 humanized mice fully derived from ES cells were available for analysis within 4 mo following gene targeting. We used this model to demonstrate that the identified antibodies can prophylactically protect mice from infection as well as ameliorate a previously established infection in a post-inoculation treatment paradigm. As such, these two antibodies are promising candidates for prophylaxis and treatment of MERS-CoV infections. Two other mouse models have been

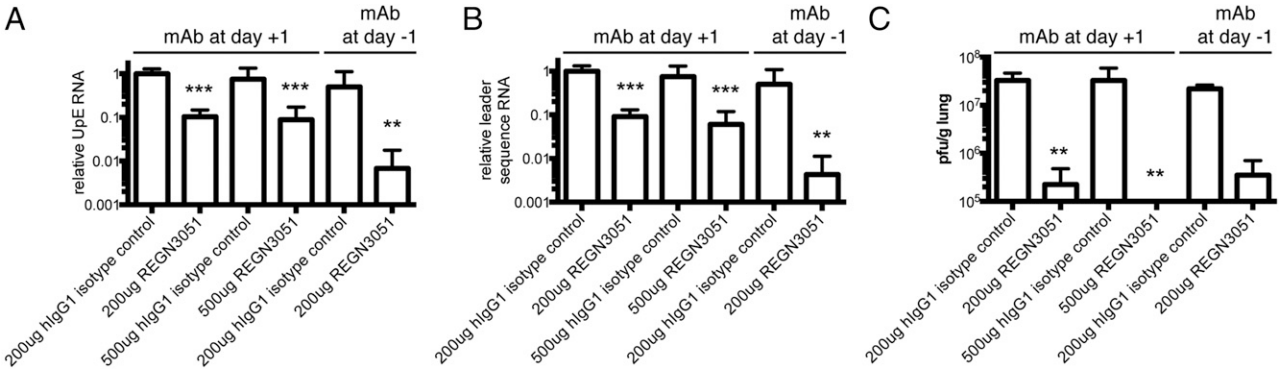

Fig. 5. In vivo treatment with anti-S antibodies 1 d after infection protects huDPP4 mice from MERS-CoV infection. Mice were intraperitoneally injected with 200 μg or 500 μg of REGN3051 or an hIgG isotype control at 1 dpi or with 200 μg of REGN3051 at 24 h preinfection. At 4 dpi, lungs were harvested and viral RNA and virus titer quantified. (*A* and *B*) Quantitative PCR of MERS-CoV transcript (*A* is MERS-CoV genome, *B* is MERS-CoV transcribed mRNA) from infected lungs was quantified using primers directed against the MERS-CoV genome and compared with hIgG1 isotype control treated mice. All samples were compared with hIgG1 control. Notice the reduction in viral RNA levels for REGN3051 treated mice given 24 h after treatment compared with levels of isotype control treated mice ($n = 5$ mice per time point and quantitative PCR performed in triplicate). (*C*) Analysis of viral titer in the lungs quantitated by plaque assay reported as plaque-forming unit per gram lung ($n = 5$ mice per time point and titers performed in triplicate). $^{**}P < 0.01$, and $^{***}P < 0.001$.

developed for MERS-CoV. The first model used an adenovirus delivery of huDPP4 intranasally into a mouse, resulting in many cells expressing the huDPP4 receptor and efficient MERS-CoV replication. However, a concern with this model is that cells not natively expressing DPP4 will be infected and the role of a broader infection of cell types may alter pathogenesis (21). More recently another model has been published where huDPP4 is under the control of the constitutively expressing chicken β-actin promoter, driving expression of huDPP4. In this model, all cells of the mouse express huDPP4, a nonphysiological expression pattern, and these mice develop extensive brain infection of MERS-CoV and rapidly succumb to infection (23). Our model replaces the mDPP4 ORF with the huDPP4; thus, the newly knocked-in huDPP4 is under the control of the endogenous mDPP4 promoter, ensuring correct physiological expression of the knocked-in gene, providing a more physiological model of human disease. Further characterization of this model will allow us to understand the host response to MERS-CoV. Additionally, the huDPP4 mouse model can also be used for the efficient testing of drugs and vaccines in a small animal model, allowing for rapid identification of additional therapeutics to identify leads for testing in nonhuman primates before they are proposed for use in humans.

The development of this model and monoclonal antibodies to MERS-CoV S show that rapid mouse model production is possible using the VelociGene technology. This technology could be applied to numerous other emerging pathogens once the species-determining factor that limits host range has been identified. The rapid identification, purification, and testing of monoclonal antibodies from the VelocImmune system (37, 38) allowed for the production of antibodies that are >1 log better inhibitors compared with other published antibodies developed with conventional approaches. The rapid identification, within several weeks, of potent monoclonal antibodies described in this study suggests that these technologies form the basis for a rapid response to address the public threat resulting from emerging coronaviruses or other pathogens that pose a serious threat to human health in the future.

Methods

Detailed information about generation and purification of anti–MERS-CoV Spike monoclonal antibodies, screening and characterization of antibody in vitro binding and neutralization properties, generation of huDPP4 mice, and testing antibodies in vivo can be found in *SI Methods*. All animal experiments were approved by The University of Maryland at Baltimore Institutional Animal Care and Use Committee.

1. Zaki AM, van Boheemen S, Bestebroer TM, Osterhaus ADME, Fouchier RAM (2012) Isolation of a novel coronavirus from a man with pneumonia in Saudi Arabia. *N Engl J Med* 367(19):1814–1820.
2. Coleman CM, Frieman MB (2013) Emergence of the Middle East respiratory syndrome coronavirus. *PLoS Pathog* 9(9):e1003595.
3. Assiri A, et al.; KSA MERS-CoV Investigation Team (2013) Hospital outbreak of Middle East respiratory syndrome coronavirus. *N Engl J Med* 369(5):407–416.
4. Cotten M, et al. (2014) Spread, circulation, and evolution of the Middle East respiratory syndrome coronavirus. *MBio* 5(1):e01062-13.
5. Perlman S, McCray PB, Jr (2013) Person-to-person spread of the MERS coronavirus—An evolving picture. *N Engl J Med* 369(5):466–467.
6. Meyer B, et al. (2014) Antibodies against MERS coronavirus in dromedary camels, United Arab Emirates, 2003 and 2013. *Emerg Infect Dis* 20(4):552–559.
7. Perera RA, et al. (2013) Seroepidemiology for MERS coronavirus using microneutralisation and pseudoparticle virus neutralisation assays reveal a high prevalence of antibody in dromedary camels in Egypt, June 2013. *Euro Surveill* 18(36):20574.
8. Reusken CB, et al. (2013) Middle East respiratory syndrome coronavirus neutralising serum antibodies in dromedary camels: A comparative serological study. *Lancet Infect Dis* 13(10):859–866.
9. Masters PS (2006) The molecular biology of coronaviruses. *Adv Virus Res* 66:193–292.
10. Gierer S, et al. (2013) The spike protein of the emerging betacoronavirus EMC uses a novel coronavirus receptor for entry, can be activated by TMPRSS2, and is targeted by neutralizing antibodies. *J Virol* 87(10):5502–5511.
11. Raj VS, et al. (2013) Dipeptidyl peptidase 4 is a functional receptor for the emerging human coronavirus-EMC. *Nature* 495(7440):251–254.
12. Hildebrandt M, Reutter W, Arck P, Rose M, Klapp BF (2000) A guardian angel: The involvement of dipeptidyl peptidase IV in psychoneuroendocrine function, nutrition and immune defence. *Clin Sci (Lond)* 99(2):93–104.
13. Lu G, et al. (2013) Molecular basis of binding between novel human coronavirus MERS-CoV and its receptor CD26. *Nature* 500(7461):227–231.
14. Wang N, et al. (2013) Structure of MERS-CoV spike receptor-binding domain complexed with human receptor DPP4. *Cell Res* 23(8):986–983.
15. Falzarano D, et al. (2013) Treatment with interferon-α2b and ribavirin improves outcome in MERS-CoV-infected rhesus macaques. *Nat Med* 19(10):1313–1317.
16. Dyall J, et al. (2014) Repurposing of clinically developed drugs for treatment of Middle East respiratory syndrome coronavirus infection. *Antimicrob Agents Chemother* 58(8):4885–4893.
17. Adedeji AO, et al. (2014) Evaluation of SSYA10-001 as a replication inhibitor of SARS, MHV and MERS coronaviruses. *Antimicrob Agents Chemother* 58(8):4894–4898.
18. de Wilde AH, et al. (2014) Screening of an FDA-approved compound library identifies four small-molecule inhibitors of Middle East respiratory syndrome coronavirus replication in cell culture. *Antimicrob Agents Chemother* 58(8):4875–4884.
19. Du L, et al. (2013) A truncated receptor-binding domain of MERS-CoV spike protein potently inhibits MERS-CoV infection and induces strong neutralizing antibody responses: Implication for developing therapeutics and vaccines. *PLoS ONE* 8(12): e81587.
20. Coleman CM, et al. (2014) Purified coronavirus spike protein nanoparticles induce coronavirus neutralizing antibodies in mice. *Vaccine* 32(26):3169–3174.
21. Zhao J, et al. (2014) Rapid generation of a mouse model for Middle East respiratory syndrome. *Proc Natl Acad Sci USA* 111(13):4970–4975.
22. Falzarano D, et al. (2014) Infection with MERS-CoV causes lethal pneumonia in the common marmoset. *PLoS Pathog* 10(8):e1004250.
23. Agrawal AS, et al. (2015) Generation of transgenic mouse model of Middle East respiratory syndrome-coronavirus infection and disease. *J Virol* 89(7):3659–3670.
24. Smith EC, Blanc H, Vignuzzi M, Denison MR (2013) Coronaviruses lacking exoribonuclease activity are susceptible to lethal mutagenesis: Evidence for proofreading and potential therapeutics. *PLoS Pathog* 9(8):e1003565.
25. Rockx B, et al. (2010) Escape from human monoclonal antibody neutralization affects in vitro and in vivo fitness of severe acute respiratory syndrome coronavirus. *J Infect Dis* 201(6):946–955.
26. Ying T, et al. (2014) Exceptionally potent neutralization of MERS-CoV by human monoclonal antibodies. *J Virol* 88(14):7796–7805.
27. Tang X-C, et al. (2014) Identification of human neutralizing antibodies against MERS-CoV and their role in virus adaptive evolution. *Proc Natl Acad Sci USA* 111(19): E2018–E2026.
28. Malpica JM, et al. (2002) The rate and character of spontaneous mutation in an RNA virus. *Genetics* 162(4):1505–1511.
29. Smith EC, Denison MR (2013) Coronaviruses as DNA wannabes: A new model for the regulation of RNA virus replication fidelity. *PLoS Pathog* 9(12):e1003760.
30. Eckerle LD, Lu X, Sperry SM, Choi L, Denison MR (2007) High fidelity of murine hepatitis virus replication is decreased in nsp14 exoribonuclease mutants. *J Virol* 81(22):12135–12144.
31. Cotten M, et al. (2013) Transmission and evolution of the Middle East respiratory syndrome coronavirus in Saudi Arabia: A descriptive genomic study. *Lancet* 382(9909): 1993–2002.
32. Jiang L, et al. (2014) Potent neutralization of MERS-CoV by human neutralizing monoclonal antibodies to the viral spike glycoprotein. *Sci Transl Med* 6(234):234ra59.
33. Coleman CM, Matthews KL, Goicochea L, Frieman MB (2014) Wild-type and innate immune-deficient mice are not susceptible to the Middle East respiratory syndrome coronavirus. *J Gen Virol* 95(Pt 2):408–412.
34. Cockrell AS, et al. (2014) Mouse dipeptidyl peptidase 4 is not a functional receptor for Middle East respiratory syndrome coronavirus infection. *J Virol* 88(9):5195–5199.
35. Good RA, Lorenz E (1991) Historic aspects of intravenous immunoglobulin therapy. *Cancer* 68(6, Suppl):1415–1421.
36. Marasco WA, Sui J (2007) The growth and potential of human antiviral monoclonal antibody therapeutics. *Nat Biotechnol* 25(12):1421–1434.
37. Murphy AJ, et al. (2014) Mice with megabase humanization of their immunoglobulin genes generate antibodies as efficiently as normal mice. *Proc Natl Acad Sci USA* 111(14):5153–5158.
38. Macdonald LE, et al. (2014) Precise and in situ genetic humanization of 6 Mb of mouse immunoglobulin genes. *Proc Natl Acad Sci USA* 111(14):5147–5152.
39. Wang X, Stollar BD (2000) Human immunoglobulin variable region gene analysis by single cell RT-PCR. *J Immunol Methods* 244(1-2):217–225.
40. Page C, et al. (2012) Induction of alternatively activated macrophages enhances pathogenesis during severe acute respiratory syndrome coronavirus infection. *J Virol* 86(24):13334–13349.
41. Valenzuela DM, et al. (2003) High-throughput engineering of the mouse genome coupled with high-resolution expression analysis. *Nat Biotechnol* 21(6):652–659.
42. Poueymirou WT, et al. (2007) F0 generation mice fully derived from gene-targeted embryonic stem cells allowing immediate phenotypic analyses. *Nat Biotechnol* 25(1): 91–99.